Journal of Engineering Science 10(1), 2019, 25-30

JES
an international Journal

STRUCTURAL AND TRANSPORT PROPERTIES OF Yb SUBSTITUTED Co-Zn FERRITES

M. D. Hossain[1], M. A. Hossain[1], M. N. I. Khan[2] and S. S. Sikder[1*]

[1]Department of Physics, Khulna University of Engineering & Technology, Khulna-9203, Bangladesh
[2]Materials Science Division, Atomic Energy Center, Dhaka-1000, Bangladesh

Received: 30 November 2018 Accepted: 15 May 2019

ABSTRACT

Yb substituted Co-Zn ferrites with general formula $Co_{0.25}Zn_{0.75}Yb_xFe_{2-x}O_4$ (x = 0.00, 0.02, 0.04, 0.06 and 0.08) were synthesized by standard double sintering method. For each sample, 850°C was the pre-sintering and 1150°C was the sintering temperature. The structural properties and frequency dependent dielectric properties of the given ferrite samples were investigated by X-ray diffractometer and impedance analyzer. The X-ray diffraction (XRD) patterns confirm eight sharp peaks demonstrating all the samples are in cubic spinel structure with single phased. With increasing Ytterbium content the lattice parameter was increased. An important change of bulk density and X-ray density has been confirmed with increasing Yb content. The electrical properties such as dielectric constant and dielectric loss factor were decreased with increasing frequency. DC resistivity was also varied with increasing Ytterbium content. The doping of Yb^{3+} ion affects the structural properties and all the samples are promising one for high frequency application.

Keywords: *Bulk Density, Dielectric Constant, Lattice Parameter, Loss Factor, Resistivity, XRD*

1. INTRODUCTION

Ferrimagnetic materials called ferrites are very essential in today's modern technology. Very poor amount of rare earth substituted in a ferrite changed its physical, magnetic and electrical properties. The structural and electrical properties also depend on method of sample preparation, cations distribution between the octahedral and tetrahedral sites, ratio of dopent (All-Hilli *et al*., 2011; Hossain *et al*., 2017). Dielectric constant of rare earth doped ferrites is suitable for long frequency range and they have a low dielectric loss which makes them suitable for various electronic devices (Ahmed *et al*., 2003; Bharathi *et al*., 2009). Rare earth doped ferrites are widely studied by the researcher for their huge amount of applications in modern technology. Optimization of various properties of a ferrite is an important issue for the sustainable development in modern technologies. Polycrystalline Co-Zn ferrite is one of the most useful ferrites, due to their several advantages over others ferrites such as available raw materials, high resistivity, and high operating frequency (Choi *et al*., 2017; El Foulani *et al*., 2018). Co-Zn ferrite shows very useful electromagnetic properties due to their chemical and physical properties (Pradhan *et al.*, 2017). Co-Zn ferrite is the combine form of $CoFe_2O_4$ and $ZnFe_2O_4$ ferrites. $ZnFe_2O_4$ ferrite is antiferromagnetic bellow the Neel temperature and Co-ferrite shows ferromagnetism. The final combination of Co-Zn ferrite shows completely different properties of Zn-ferrite and Co-ferrite. Shivaji *et al.*, (2012) studied the rare earth Dy doped Cobalt–Zinc ferrites, synthesized by sol–gel auto combustion method. They observed that the structural and dielectric properties change with increasing the Dysprosium content in the Cobalt–Zinc ferrites. Mugutkar *et al.* (2018) reported the impact of the rare earth Gd^{3+} substitution improved of magnetization (σ_s) and decrease of coercivity (H_c) of Co-Zn ferrites. The rare earth La^{3+} ions doped in the ferrite also improved the structural properties and dielectric properties. Karimunnesa *et al*., (2018) recently investigated the magnetic, structural and transport properties of Ho^{3+} doped Co-ferrites. The authors suggested that rare earth doped Co-ferrites are very good for the high frequency range. In the present study, the aim was to detect the structure and electrical properties of $Co_{0.25}Zn_{0.75}Yb_xFe_{2-x}O_4$ ferrite samples and observe the changes in crystal phase, lattice parameter, density, porosity, dielectric constant with real and imaginary part, dielectric loss and DC resistivity etc.

2. MATERIALS AND METHOD

High purity powders of ZnO (99.9%), Co_3O_4 (98.9%), Yb_2O_3 (99.8%), Fe_2O_3 (99.8%) were used as the raw materials. The exact amounts of compounds were calculated according to their molecular weight. The raw materials were thoroughly mixed by hand milling using agate mortar for 4 hours. After hand milling, the mixture was pre-sintered at 850ºC for 2 hours. A KSL-1700X-S muffle furnace was used for pre-sintering and sintering process. The calcined powder again ground into fine powders. Then the fine powders were placed into various dies for toroid and disk-

* Corresponding Author: sssikder@yahoo.com

shaped samples. In the final stage, we sintered the samples at 1150 ^{0}C for 3 hours. After sintering the sample, we got the final product. From Figure 1, we can see the pictorial representation of the sample preparation process.

XRD was carried out by a Philips X'Pert Pro X-ray diffractometer where, the Cu - Ka radiation was used with the wavelength (λ=1.5418Å). Using the X-ray data and Nelson-Riley function Lattice parameters were determined. The X-ray density of studied samples was determined from X-ray data based lattice parameter. The bulk density of the samples was determined with the help digital weight machine and slide calipers. The measurements of dielectric constant and dielectric loss factors of the ferrite samples were performed using LCR Meter Bridge (Wayne Kerr Impedance analyzer, 6500B). DC resistivity of all the samples was measured with the help of a Kethly multimeter.

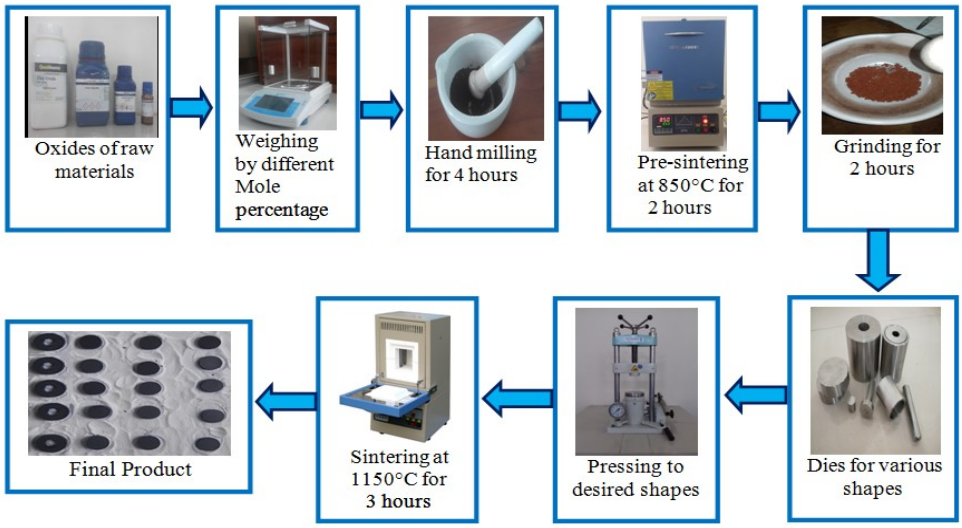

Figure 1: Sample preparation at a glance.

3. RESULTS AND DISCUSSION

3.1 X-ray Diffraction Analysis

The structural view or the various phases of Yb doped Co-Zn ferrites were confirmed from XRD analysis. The X-ray diffraction patterns of Yb doped Co-Zn ferrites are shown in Figure 1. For each of the studied samples we get eight sharp peaks and the peaks can be indexed as (111), (220), (311), (222), (400), (422), (511), and (440). No impurity peak is found and all the Miller indices of a peak are either all odd or even, which confirmed that the Yb doped Co-Zn ferrite samples are spinel lattice with cubic structure. This also confirms the homogeneity of the studied samples.

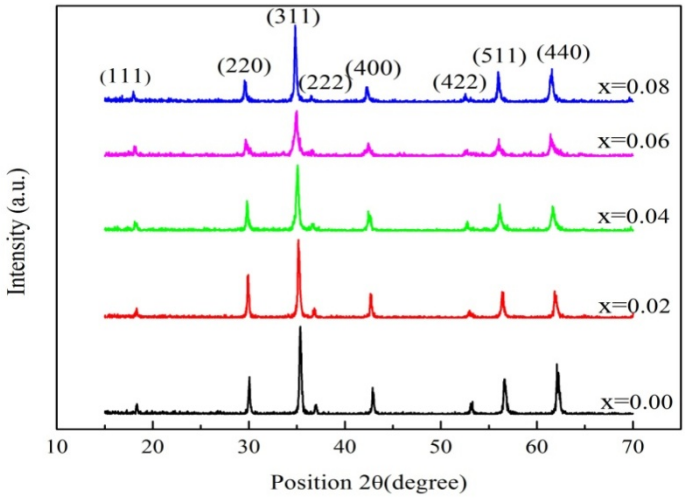

Figure 2: X-ray diffraction spectra of $Co_{0.25}Zn_{0.75}Yb_xFe_{2-x}O_4$, [x=0.00, 0.02, 0.04, 0.06 and 0.08] ferrites sintered at 1150 °C for 3 hours.

From the X-ray data, we calculated the position of any peaks and using Bragg's law ($2d \sin\theta = n\lambda$) we got the values of interplanar spacing (d). The position of the X-ray peaks and Miller indices of the planes of the ferrite samples are given in Table 1.

Table 1: Position of the X-ray peaks and Miller indices of the planes of $Co_{0.25}Zn_{0.75}Yb_xFe_{2-x}O_4$ [x=0.00, 0.02, 0.04, 0.06 and 0.08] ferrites.

Content	Miller indices of the X-ray peaks and their position 2θ in degree							
	(111)	(220)	(311)	(222)	(400)	(422)	(511)	(440)
X=0.00	18.35	30.02	35.36	36.9	42.9	53.21	56.63	62.05
X=0.02	18.29	29.91	35.13	36.83	42.67	52.95	56.40	61.83
X=0.04	18.16	29.78	35.06	36.68	42.47	52.74	56.12	61.62
X=0.06	18.10	29.64	34.98	36.60	42.39	52.70	56.00	61.43
X=0.08	17.97	29.52	34.81	36.50	42.3	52.55	55.99	61.58

3.2 Lattice Parameters

The lattice parameters of the Yb doped Co-Zn ferrites were calculated with the help of interplanar spacing (d) and Miller indices (h, k, l). We also used Nelson-Riley extrapolation method for exact lattice parameter. We plotted the values of lattice parameter with respect to all the XRD peaks against Nelson-Riley function. The N-R function, F(θ) can be written as $F(\theta) = \frac{1}{2}\left[\frac{cos^2\theta}{sin^2\theta} + \frac{cos^2\theta}{\theta}\right]$, Where θ is the Bragg's angle, by extrapolating lattice parameter's values of F (θ) = 0 or θ = 90°. For each of the reflection plane, we got an individual F (θ) and individual lattice parameter.

For every sample we got different lattice parameters for different N-R functions as shown in Figures 3(a-e). Then for average lattice parameter we used square linear fitting which gives an intercept on the Y-axis.

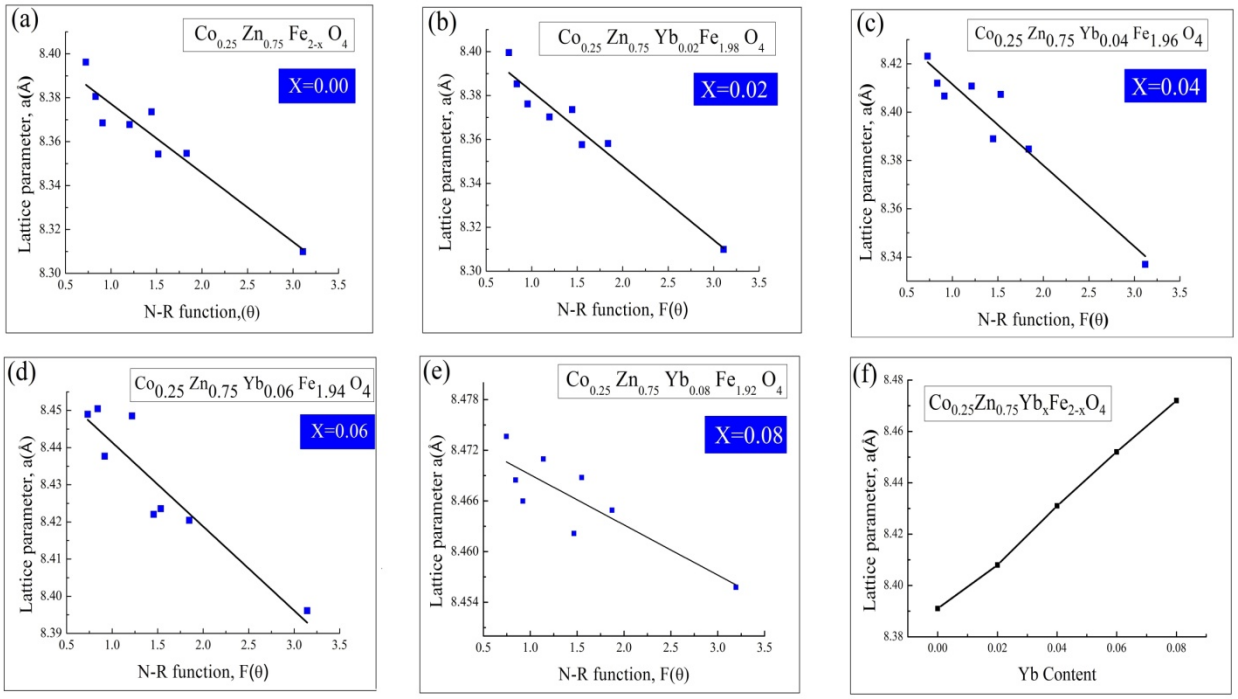

Figure 3: (a-e) Lattice parameters with N-R function and (f) Change in lattice parameter with Yb content.

From Figure 3(f) it is clear that the lattice parameter (a) increases with increasing Yb^{3+} content. This increase in lattice constant can be described with the concept of ionic radii. The ionic radii of the cations used in the given $Co_{0.25}Zn_{0.75}Yb_xFe_{2-x}O_4$ samples are Co^{2+}(0.72 Å), Zn^{2+}(0.82 Å), Yb^{3+} (1.03Å) and Fe^{3+} (0.64Å). Here the ionic radius of Yb is greater than the ionic radii of Fe. For this reason doping of big atom increases the lattice parameter and these changes in lattice parameters with Yb content indicate that the present ferrite samples follow the Vegard's law (Vegards, 1921).

3.3 Density and Porosity

Density and porosity are the important variables which affect the structural, electrical and many other properties of a ferrite sample. When we calculated the density with the help of XRD data then the density is called X-ray density. Mathematical expression for X-ray density can be written as, $\rho_x = \frac{8M}{Na^3}$, where M is molecular weight, N is Avogadro's number, a^3 is volume of the unit cell and 8 is the number of atoms in a unit cell. The bulk density was calculated from, $\rho_B = \frac{m}{\pi r^2 h}$, where r is radius, m is mass and h is the height of the pellet sample. The calculated values of the X-ray or theoretical density (ρ_x), bulk density (ρ_B) and porosity (P %) of the present ferrites are listed in Table 2. The theoretical density was increased from 5.38 to 5.44 g/cm^3 with increasing Yb^{3+} content. We know that ρ_x depends on the lattice constant (a) and molecular weight (M) of the sample. For this reason, this increase in ρ_x might be responsible for the greater atomic mass of Ytterbium (173.04 amu) than Iron (55.85 amu).

Table 2: Lattice parameter (a), X-ray density (ρ_x), bulk density (ρ_B), porosity (P %) of $Co_{0.25}Zn_{0.75}Yb_xFe_{2-x}O_4$ ferrites sintered at 1150 °C for 3 hours.

Content	Lattice parameter in (Å)	ρ_x in (gm/cm^3)	ρ_B in (gm/cm^3)	Porosity (%)
X= 0.00	8.391	5.38	4.99	7.13
X= 0.02	8.408	5.40	4.96	8.13
X= 0.04	8.431	5.41	4.92	8.90
X= 0.06	8.452	5.42	4.88	9.94
X= 0.08	8.472	5.44	4.82	11.30

It is cleared that X-ray density is greater than bulk density as shown in Figure 4(a). This phenomenon can be explained with the existence of pores in the ferrite samples. Basically, the pores were shaped and evolved during the sample preparation process (Shil *et al*., 2012). The bulk density slightly decreases with increasing rare earth ion Yb^{3+} and the X-ray density rises gradually with increasing Yb content.

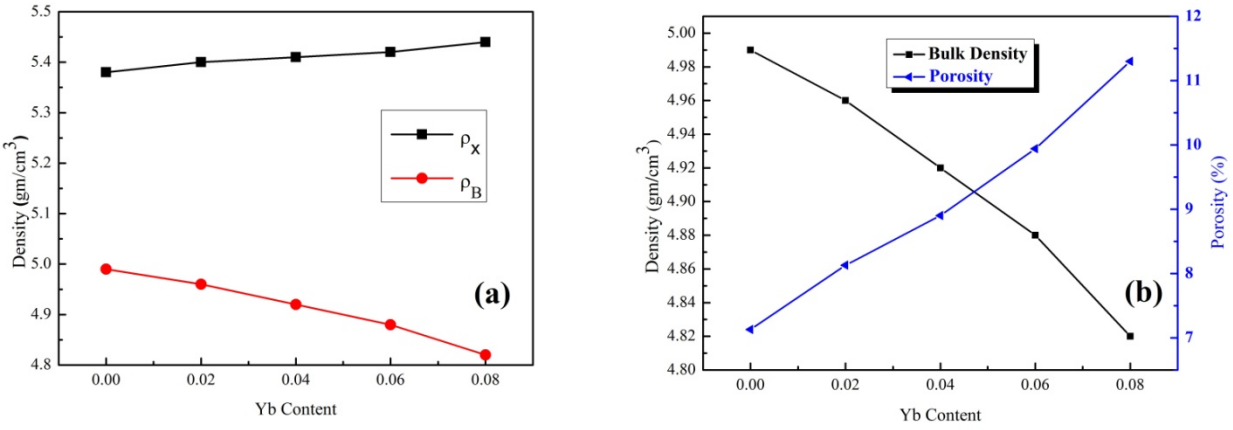

Figure 4: (a) Variation of bulk density and X-ray density as a function of Yb content, (b) Relationship between bulk density and porosity with Yb content

Figure 4(b) shows the porosity rises with increasing Yb^{3+} content. Here the porosity determines the ratio between void density and theoretical density. The total porosity depends on inter granular porosity, intra granular porosity and grain size (Yang *et al.,* 2006). The decrease of bulk density increases the porosity, which creates the inverse relationship between bulk density and porosity.

3.4 Frequency Dependent Dielectric Constant

The frequency dependence real part and the imaginary part of the dielectric constant are shown in Figures 7(a-b). For all the samples ε' was decreased with the increase in frequency. This phenomenon depends on interfacial polarization which can be discussed by the Maxwell Wagner model. According to this model, dielectric materials contain conductive grains detached by highly resistive interface between two grains. Polarization of Yb doped Co-Zn ferrite was occurring due to the hopping of electrons in various oxidation stages between ions of the common element

(Verma *et al*., 2005). For an applied external field the electrons move towards the direction of the field at the same time electrons stack up the crystal boundaries then the polarization occurs. The electrons cannot balance with the field in a higher frequency range. For this reason, the polarization decreases with rising frequency and hence the dielectric constant decreases. This type of ferrites with lower dielectric constant can be used in high frequency devices.

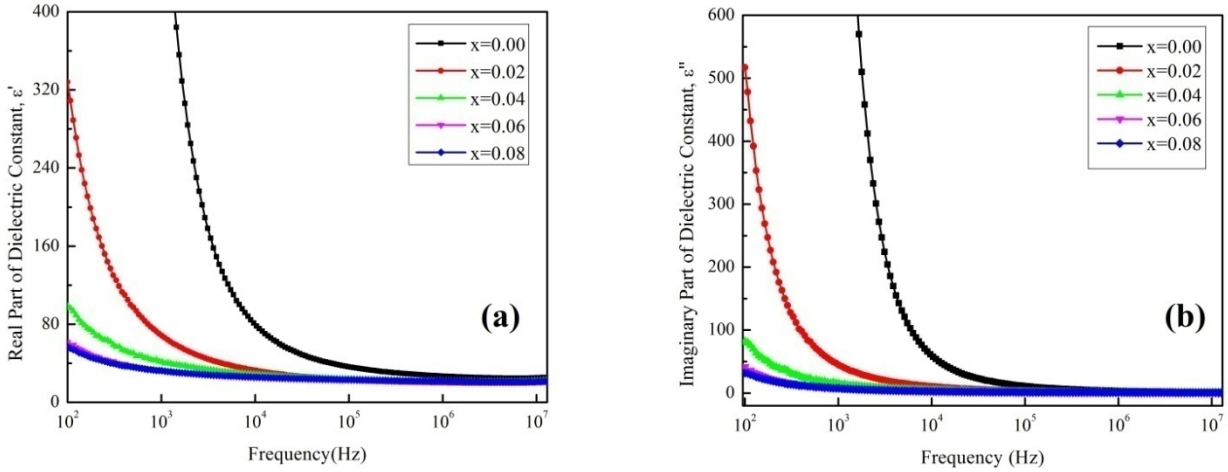

Figure 5: Frequency dependent (a) real part of dielectric constant and (b) imaginary part of dielectric constant of $Co_{0.25}Zn_{0.75}Yb_xFe_{2-x}O_4$ $[x = 0.0, 0.02, 0.04, 0.06\ and\ 0.08]$ ferrites sintered at 1150°C for 3 hours.

3.5 Dielectric Loss and Resistivity

Figure 6(a) shows the normal behavior of dielectric loss with frequency, loss tangent declines with increasing frequency. In low frequency region the dielectric $\tan \delta_E$ decreases rapidly on the other hand the rate of decrease was very slow in high frequency region. In the low frequency region, electrons need more energy to exchange between Fe^{2+} and Fe^{3+} due to more resistance in the grain boundary which becomes the higher dielectric loss. The electrons need small energy to exchange between Fe^{2+} and Fe^{3+} in the high frequency region for low resistivity (due to grains). For this reason, dielectric loss becomes almost constant in high frequency.

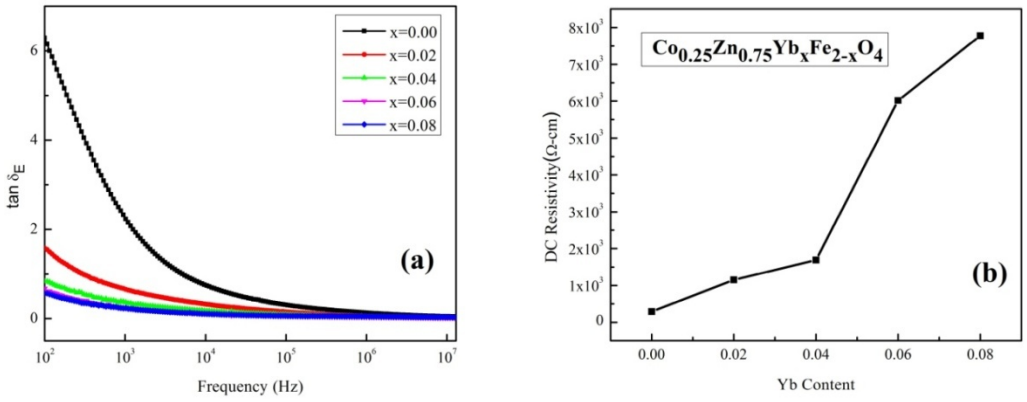

Figure 6: (a) Frequency dependent dielectric loss and (b) Variation of DC resistivity with Yb content.

From Figure 6(b) we can see that DC resistivity increases rapidly with increasing Yb content. We can explain this phenomenon by the hopping mechanism of Verway (Verway *et al*., 1936). From this mechanism, hopping of electrons between Fe^{2+} and Fe^{3+} ions of the same element create electrical conduction. Without Yb content the concentration of the iron is found maximum at B-site. When the Yb content increased in A-site, a decrease of Fe ion observed in B-site. Here some Fe^{3+} ion shifted from A to B site to balance the increased amount of Yb ions at A-sites. For this reason, electron hopping between Fe^{2+} and Fe^{3+} is greater at B-site. As iron replaced by Yb^{3+} ion and Yb^{3+} ion is nonconductive than Fe^{3+} ion, which is responsible for increasing the DC resistivity of the studied samples.

4. CONCLUSIONS

According to the above results, it is proved that the Yb doped Co-Zn ferrites show a significant change in structural and electrical properties. The increase in lattice parameter with increasing Yb content ensures the change in crystal structure. The decrease of dielectric constant and dielectric loss tangent are higher at low frequency and it becomes independent at higher frequency region. These properties make them a good candidate for inductive materials and higher frequency application. DC resistivity has been observed arising tendency due to increasing the porosity and lattice parameter of the samples with Yb content, which is better for structural and dielectric properties.

ACKNOWLEDGEMENT

The authors gratefully acknowledge the Material Science Division, Atomic Energy Centre, Dhaka, Bangladesh for XRD measurements.

REFERENCES

Ahmed, M. A., Ateia E., and El-dek S. I., 2003. Rare earth doping on the structural and electrical properties of Mg-Ti ferrite, *Materials letters*, 57, 4256-4266.

Al-Hilli Muthafar, Sean Li and Kassim S. K., 2011: Gadolinium substitution and sintering temperature dependent electronic properties of Li-Ni ferrite, *Materials chemistry and Physics*, 128, 127-132.

Bharathi, K. K., Chelvane J. A., and Markandeyulu G., 2009. Magnetoelectric properties of Gd and Nd-doped nickel ferrite, *J. Magn. Magn. Mater*, 321, 3677-3680.

Choi, H., Lee S., Kouh T., Kim S. J., Kim C. S., and Hahn E., 2017. Synthesis and characterization of Co-Zn ferrite nanoparticles for application to magnetic hyperthermia. *Journal of the Korean Physical Society*, *70*(1), 89-92.

El Foulani, A. H., Pullar R. C., Amjoud M., Ouzaouit K., and Aamouche A., 2018. Magnetic and Nanostructural Properties of Cobalt–Zinc Ferrite for Environmental Sensors. *Handbook of Environmental Materials Management*, 1-18.

Hossain M. A., Khan A. K. M., and Sikder, S. S., 2017. Structural magnetic and dielectric behaviors of Y^{3+} substituted Ni-Zn ferrites, *Int. J. of Nano Science Trends and Tech.*, 1.2, 1-19.

Karimunnesa, S., Atique Ullah A. K. M., Hassan M. R., Shanta F. S., Islam R., and Khan M. N. I., 2018. Effect of holmium substitution on the structural, magnetic and transport properties of $CoFe_{2-x}Ho_xO_4$ ferrites, *Journal of Magnetism and Magnetic Materials,*457, 57-63.

Mugutkar, A. B., Gore S. K., Mane R. S., Batoo K. M., Adil S. F., and Jadhav S. S., 2018. Magneto-structural behaviour of Gd doped nanocrystalline Co-Zn ferrites governed by domain wall movement and spin rotations. *Ceramics International*, *44*(17), 21675-21683.

Pradhan, A. K., Mandal P. R., Bera K., Saha S., and Nath T. K., 2017. The effect of Mo doping on the structural and dielectric properties of Co-Zn ferrite. *Physica B: Condensed Matter*, *525*, 1-6.

Shil, S. K., Sinha R. C., Hakim A. K. M., and Sikder S. S., 2012. Influence of composition and sintering temperature on magnetic and electrical properties of spinel type Ni-Zn ferrite. *Jahangirnagar University Journal of Science*, 35, 23-36.

Shivaji, R. K., Sanjay S. K., Pramod N. J., Vashishtha M. G., Duryodhan P. W., Govind B. K., Sandip R. S., and Sambhaji R. B., 2012: Synthesis of Dy doped Co–Zn ferrite by sol–gel auto combustion method and its characterization, Materials *Letters*, 84, 169 – 172.

Vagards, L., 1921: Die constitution der mischkristalle und die raumfullung der atome, *Z. Physics*, 5, 17.

Verma, A., Thakur O. P., Prakash C., Goel T. C., Mendiratta R. G., 2005. Temperature dependence of electrical properties of nickel-zinc ferrites processed by the citrate precursor technique, *Mater. Sci. Eng*., 116, 1-6.

Verway, E. J. W., Heilmann E. L. J., and Romeijin F. C., 1947. Physical Properties and Cation Arrangement of Oxides with Spinel Structure, *J. Chem. Phys.,* 15 (4), 181 - 187.

Yang, Z. H., Gong, Z. Q., Li, H. X., Ma, Y. T. and Yang, Y. F., 2006. Synthesis of Ni-Zn Ferrites and Its Microstructure and Magnetic Properties, J*ournal of Central South University of Technology*, 13, 618-623.